A Surface Micromachined Electrostatic Ultrasonic Air Transducer

Matthew I. Haller* and Butrus T. Khuri-Yakub
E.L. Ginzton Laboratory
Stanford University
Stanford, CA 94305

* Currently at Acuson Corporation
1350 Shorebird Way
Mountain View, CA 94039

Abstract

Electrostatic transducers have long been used for audio speakers and as capacitance receivers. In this paper, we describe a technique to fabricate an electrostatic transducer using silicon surface micromachining. Using these techniques to fabricate arrays of transducers with small electrode spacing, we make efficient and broadband ultrasonic air transducers. These transducers are made using standard silicon processing techniques allowing them to be integrated, in the future, with control electronics for the fabrication of electronically scanned systems with large transducer arrays. The air transducer described in this paper operates at 1.9 MHz with an insertion loss of 26 dB (slightly worse than a reference piezoelectric transducer) and a 20% bandwidth (~4 times better than the piezoelectric transducer). The impulse response of the transducer has a short ringdown time due to the fact that the transducer has a single resonance. We present here the theory of operation, the fabrication technique used, and the characterization of the device. Electrical, optical and acoustic measurements were preformed and compared with theory. In all cases, the measurements agree very well with theory.

I. Introduction

Electrostatic transducers have long been used for audio speakers[1] and as capacitance receivers[2]. In this paper, we describe a technique to fabricate an electrostatic transducer using silicon surface micromachining. Silicon processing techniques have developed over the last few decades enabling precise control over structures on a nanometer scale. Using these techniques to fabricate arrays of transducers with small electrode spacing, we make efficient and broadband ultrasonic air transducers. These transducers are made using standard silicon processing techniques allowing them to be integrated, in the future, with control electronics for the fabrication of electronically scanned systems with large transducer arrays.

The air transducer described in this paper operates at 1.9 MHz with an insertion loss of 26 dB (slightly worse than a reference piezoelectric transducer) and a 20% bandwidth (~4 times better than the piezoelectric transducer). The impulse response of the transducer has a short ringdown time due to the fact that the transducer has a single resonance.

We describe the theory of operation of the electrostatic air transducer. This theory was first developed by Mason[2], and is extended here to account for the particular geometry of the fabricated device. Additionally, parasitic effects that were not present in the Mason's work. re included in the model. The fabrication techniques used are described as well as the measured performance of the transducer. The measurements agree very well with theory.

II. Theory of Operation

Consider a parallel plate capacitor with one fixed and one free electrode. If a voltage V is applied to the capacitor, the free electrode will experience an attractive electrostatic force of magnitude:

$$F = \frac{1}{2}\varepsilon A\frac{V^2}{d^2} \tag{1}$$

Where ε is the dielectric constant of the material between the plates, A is the capacitor area, and d is the electrode spacing. A large force is applied to the free electrode if 'V' is increased or if 'd' is decreased. Because the force depends on the square of the voltage, the second harmonic of the applied voltage will be generated. For operation at the first harmonic, a DC bias V_{bias} is applied to the capacitor along with the RF signal such that:

$$V(t) = V_{bias} + V_{ac}\cos(\omega t + \phi) \tag{2}$$

Then, the applied force will be:

$$F = \frac{\varepsilon A}{2d^2}\left(V_{bias}^2 + 2V_{bias}V_{ac}\cos(\omega t + \phi) + V_{ac}\cos^2(\omega t + \phi)\right) \tag{3}$$

By making the bias voltage much larger than the time varying voltage, the dominant time varying force becomes:

$$F = \frac{\varepsilon A V_{bias}V_{ac}}{d^2}\cos(\omega t + \phi) \tag{4}$$

A good design requires a large linear displacement due to the applied voltage so that a large amount of ultrasonic energy is coupled into the air.

Consider a circular membrane suspended above a rigid back plate (as shown in Figure 1).

Figure 1. Schematic of nitride membrane attracted to substrate by an electrostatic force.

Following Mason's analysis[2], we can write the equation of motion of the membrane in phasor terms (assuming $e^{j\omega t}$ time variation) as shown in equation (5). The first term of the left hand side of the equation is the restoring force of the membrane, the second term is the inertial force of the membrane element and the third term is the electrostatic force.

$$\sigma_0 t_n\left(\frac{d^2u}{dr^2} + \frac{1}{r}\frac{du}{dr}\right) + \omega^2\rho t_n u + P = 0 \tag{5}$$

Where σ_0 is the residual stress in the membrane, t_n is the membrane thickness, r is the radial position measured from the center, u is the membrane displacement as a function of r, ω is the radian frequency of the drive voltage, ρ is the membrane density and P is the electrostatic pressure applied to the membrane:

$$P = \frac{\varepsilon_{eff}V_{bias}V_{ac}}{d_{eff}^2}, \text{ where } \frac{\varepsilon_{eff}}{d_{eff}^2} = \frac{\varepsilon_a\varepsilon_n}{(t_a + t_n)(\varepsilon_a t_n + \varepsilon_n t_a)} \tag{6}$$

Where ε_{eff} is the effective dielectric constant and d_{eff} is the effective spacing of the series combination of the membrane (silicon nitride) and air gap. ε_a and ε_n are the dielectric constants of air and silicon nitride respectively, and t_a is the air gap thickness.

The solution to (5) can be found for a circular membrane of radius a to be:

$$u(r) = \frac{P}{\omega^2\rho t_n}\left[\frac{J_0(kr)}{J_0(ka)} - 1\right], \text{ where } k = \omega\sqrt{\frac{\rho}{\sigma_0}} \tag{7}$$

Where $J_0(x)$ is the zeroth order Bessel function. This has a peak displacement at resonance when $\omega = \omega_0 = 2.405\frac{2\pi}{a}\sqrt{\frac{\sigma_0}{\rho}}$. If we consider an array of circular membranes vibrating in unison, the average velocity at the surface will be given by:

1051-0117/94/0000-1241 $4.00 © 1994 IEEE

(8) $$v_{average} = \frac{2j\omega\alpha}{a^2}\int u(r) r dr$$

Where α is the fraction of the surface that is a vibrating membrane (the other regions are rigid).

The effective mechanical impedance (Z_m) of the membrane can then found to be:

(9) $$Z_m = \frac{P}{v_{average}}$$

Combining (6), (7), and (8) we can solve (9) to find:

(10) $$Z_m = \frac{-j\omega\rho t_n k a J_0(ka)}{\alpha\left[2J_1(ka) - kaJ_0(ka)\right]}$$

Where $J_1(x)$ is the first order Bessel function. This equation gives the mechanical impedance of an array of circular membranes as a function of frequency and its physical properties. Using this equation, we can find an equivalent circuit for the transducer as described in the next section.

The resonant frequency of the membrane is given by

(11) $$f_0 = \frac{2.405}{a}\sqrt{\frac{\sigma_0}{\rho}}$$

Which means that the wavelength in air will be:

(12) $$\lambda_{air} = \frac{c_{air}}{f_0} = a\frac{c_{air}}{2.405}\sqrt{\frac{\rho}{\sigma_0}}$$

For the case when σ_0=280 MPas and ρ=2861 kg/m^3, $\lambda_{air} \approx \frac{a}{2}$. Thus, the diameter of the membrane is approximately four times the wavelength of the sound in air. The Fresnel parameter of a single membrane then becomes[9]:

(13) $$S = \frac{z\lambda}{a^2} = \frac{z\frac{a}{2}}{a^2} = \frac{z}{2a}$$

This indicates that the far field of an individual membrane is at a distance equal to the diameter of the membrane away. This will typically be on the order of a few hundreds of microns.

It is now possible to determine the equivalent circuit for the transducer as a mechanical impedance, coupled through a transformer, to the electrical port as demonstrated by Mason[6], and as seen in Figure 2.

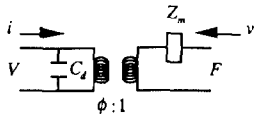

Figure 2 Equivalent circuit of electrostatic membrane transducer. Note: This is an idealized model with no losses.

The force at the acoustic port can be written as the sum of the electrostatic pressure (P) times the effective area plus the surface velocity times the mechanical impedance of the membrane:

(14) $$F = \alpha AP + Z_m v$$

If we set the current to zero and clamp the acoustic port (setting $v = 0$), then we can relate the voltage across the transformer (V_{ac}) and the force at the acoustic port by the transformer ratio:

(15) $$V_{ac} = \phi F = \phi\alpha AP$$

The transformer ratio is then given by (using Equation 6):

(16) $$\varphi = \frac{V_{ac}}{\alpha AP} = \frac{d_{eff}^2}{\alpha\varepsilon_{eff} V_{bias} A}$$

The capacitance of the active membrane elements is given by C_d:

(17) $$C_d = \alpha A\frac{\varepsilon_{eff}}{d_{eff}}$$

This equivalent circuit is used to find the electrical impedance, the particle displacement, and the insertion loss of the device.

III. Device Fabrication

The first step in fabricating the transducers is to start with highly doped, p-type, <100>, single side polished, 4" silicon wafers as a substrate. The next step is to grow a 1 μm layer of thermal oxide, followed by the deposition of a 7500 Å thick layer of low stress LPCVD silicon nitride. This nitride had a measured residual stress of 280 MPas[6]. This value can be adjusted by varying the proportion of silane to ammonia during the deposition stage. The backside of the wafer is stripped of these layers, and a 500 Å film of gold is evaporated onto both sides of the wafer. A pattern of 3 μm diameter dots on a 2 dimensional grid with 100 μm period (other samples with 50 μm and 25 μm periods were also prepared) is transferred lithographically to the wafer. The gold and the nitride were etched through the holes, leaving access to the silicon dioxide, which acts as a sacrificial layer. The wafer is then diced to 1 cm x 1 cm square samples for ease of handling. The sacrificial layer is then etched by pure hydrofluoric acid during a timed etch. This entire fabrication process is shown schematically in Figure 3.

The layer thicknesses, thin film stresses and membrane dimensions described above were chosen for a variety of reasons. One major consideration was the prevention of the membrane sticking to the substrate. To prevent the membrane from sticking, we need to have a residual stress in the membrane. This force is equal to the first term of equation (5). At the center of the membrane, with the membrane touching the silicon substrate, this force is equal to:

(18) $$Force \propto \frac{t_{oxide} t_{nitride} \sigma_0}{a^2}$$

This force is counter balanced by the Van der Wals force exerted between the membrane and the substrate which is proportional to the membrane area (or the square of the radius). The resonant frequency of the transducer is given in equation (11) and is a function of the membrane radius, the residual stress and the density of the membrane. From equation (4) and (6) we see that electrostatic force increases as we decrease the oxide and nitride thicknesses. The thinner that we make the oxide and nitride layers, the larger the electrostatic force and the greater the sticking problem. It is possible to compensate for this by increasing the residual stress in the nitride. However, if the stress is over approximately 1 GPa, the membrane will break. To improve the reliability of the process, a membrane stress of 280 MPas was chosen. Additionally, the peak displacement of the membrane will be limited by the oxide thickness. Thus, given these design considerations, the values, stated earlier were chosen.

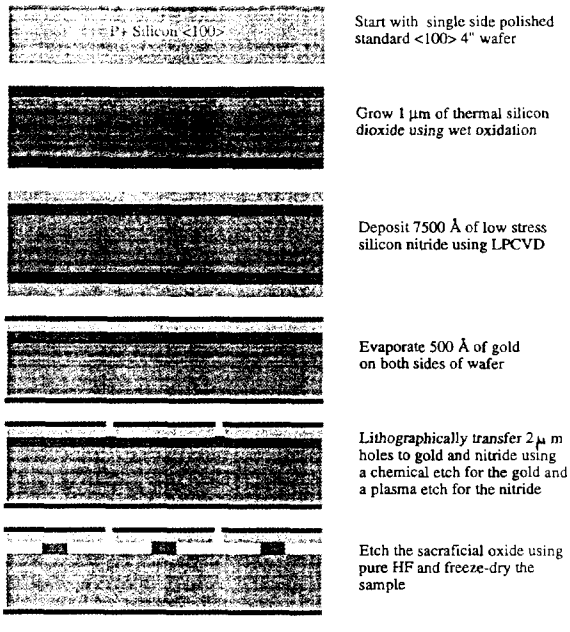

Figure 3. Process flow to fabricate the electrostatic transducer using a single mask, self-aligned, timed etch process.

The last step in the process is a timed chemical etch. Pure hydrofluoric acid etches thermal silicon dioxide at approximately 2 μm per minute. This rate, however, is time dependent since for longer etches, the fluorine ions need to diffuse longer through the small nitride opening. We find that etching for 41 minutes for the devices with a hole period of 100 μm leaves posts of silicon dioxide (approximately 20 x 20 μm) that serve to support the membrane without consuming much of the active area of the device. A cross section of an actual device is shown in Figure 4.

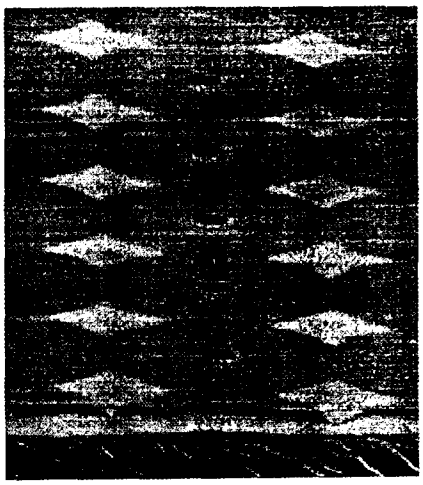

Figure 4 SEM cross-section of a 25 μm period electrostatic source. The white diamond regions are the oxide posts acting as spacers to the nitride membrane.

We fabricated several devices with periods of 100, 50 and 25 μm. The SEM of Figure 4 is of a 25 μm period device. Our interest was in devices that operated in the 1-2 MHz range. The 100 μm devices were most efficient at 1.8 MHz, as expected, so most of the measurements were performed on these devices. The silicon dioxide posts provide the lateral clamping of the silicon nitride membrane. Thus, their period determines the resonant frequency of the device. The length of the timed etch determines the size of the membrane elements.

After the sample has been fabricated, electrical contact is made to the front and back surfaces of the transducer using a ball bonded bold wire. The silicon sample is then bonded to a fixture suitable for experimentation.

This fabrication technique is limited to making either circular membranes. We can also make membranes of arbitrary shapes by confining the sacrificial etch. This is done by isolating regions of silicon dioxide using silicon nitride ridges. Thus, the structure shape is not determined by a timed etch but by lithography.

IV. Results

The performance of the devices was compared against theoretical predictions using the equivalent circuit of Figure 2. The first measurement was of the electrical impedance of the transducer which was done using an H-P impedance analyzer with a dc bias of 40 V. The transducer measured was a 50 μm period device with a resonant frequency of 4.5 MHz. Using Figure 2, the theoretical impedance is compared against the measured data in Figure 5. The values used to calculate the theoretical impedance of the device are listed in Table 1.

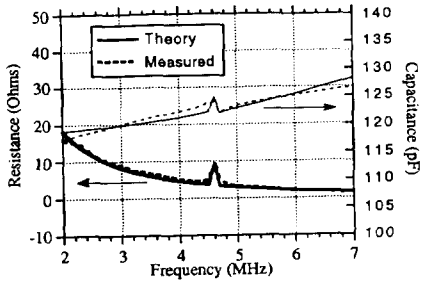

Figure 5 Measured and theoretical electrical impedance as a function of frequency for a 50 μm period device.

Variable	Value	Method
t_n	7500 Å	Measured from SEM
ρ_n	2861 kg/m^3	Fit to data
ϵ_n	4.1 • 10^{-11} F/m	Published
a	26 μm	Measured from SEM
V_{bias}	40 Volts	Measured
σ	280 MPas	Measured
α	0.55	Measured from SEM
Area	(2.5 x 2.5) mm^2	Measured
Rs	50 Ohms	Measured

Table 1. List of values used for the model of (Figure 2) to calculate the theoretical impedance in Figure 5.

We see excellent agreement between the measured data and the theoretically predicted response. This indicates that the equivalent circuit is accurate for modeling the transducer performance.

The surface displacement of the transducer was measured by an optical interferometer developed by Chung-Kao Peter Hsieh[7]. In this measurement system, an optical probe reflects off of the transducer face and interferes with a reference beam causing a time varying interference signal. A complete description of the system can be found in the literature[8] and this kind of system has been shown to give sub-Å resolution.

The surface displacement of the 100 μm transducer is shown in Figure 6 along with the comparison of the measured data and its comparison to theory. Again, we see excellent agreement with theory. The peak displacements of the 100 μm transducer was 230 Å/V. This is a very large displacement as compared with what is typical for piezoelectric transducers. It is important to remember that this displacement is measured at the center of the transducer where the displacement is maximum. The average displacement will be approximately 30% lower.

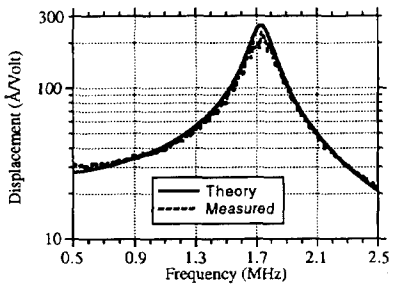

Figure 6 Measured and theoretical peak displacement for the 100 μm period device with 100 V bias.

The most important demonstration of the electrostatic transducer is to both generate and detect sound in air. We have proven that the membranes vibrate and thus generate sound using the laser interferometer. Ultrasonic detection is done by applying a voltage across the transducer, insonifying the membrane and measuring the generated current. Since the membrane is a capacitor, as the membrane is vibrated, its capacitance will change, thus acting as a current source. By using a high impedance amplifier, this signal can be detected and a complete transmit-receive system is constructed. A schematic of this system is shown in Figure 7.

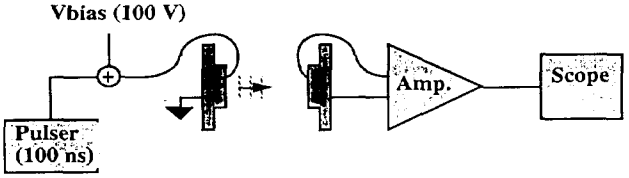

Figure 7. Schematic of acoustic measurement system.

With the transducers separated by 1 cm, the signal shown in Figure 8 is detected with a signal to noise ratio of 34 dB. This signal is very compact with little ringing.

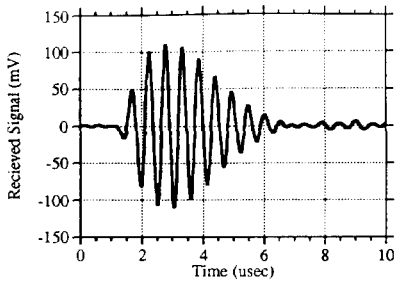

Figure 8 Received signal for experiment shown in Figure 7 with a transducer separation of 1 cm.

By taking a Fourier transform of this signal, we can get the frequency response of the transducer. It is necessary to correct for the transfer function of the amplifiers (a small effect), diffraction and acoustic losses in the air:

(19) $$Loss = 1.2(dB/cm)f(MHz)^2$$

We can then compare the frequency response with the theoretically predicted response from Figure 2 as shown in Figure 9. The 3 dB bandwidth is about 350 kHz which corresponds to a 20% bandwidth. This is considerably larger than what is achievable with conventional piezoelectric air transducers.

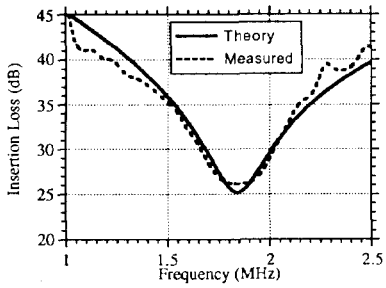

Figure 9. One way insertion loss (measured and theoretical) of the 100 μm period devices with 100 V bias voltage.

Note the very short pulse length. This is the shortest pulse reported in the literature for this excitation area at this frequency. These devices were operated with a bias voltage of 100 V across a 1 μm gap. The reason that we are able to do this is that the breakdown voltage increases as we decrease the gap size.

Figure 10 shows how much the breakdown voltage increases as well as where our device operates.

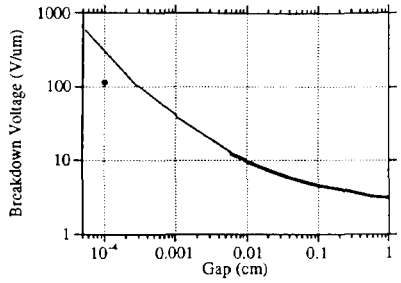

Figure 10. Breakdown field as a function of gap spacing.

The measured performance of the electrostatic transducer agreed very well with the theory predicted by the equivalent circuit and exhibited excellent bandwidth and efficiency. Some other issues that effect their usefulness is discussed in the next section.

V. Summary

In this paper, we have described the theory of operation, fabrication and measurement of a surface micromachined ultrasonic transducer operating in air. This transducer offers many advantages over conventional piezoelectric transducers. Due to the small electrode spacing that we have obtained, the efficiency of our device was comparable to piezoelectric sources. The single resonance of the silicon nitride membrane gave a short impulse response and a broad bandwidth. This is very important for many airborne ultrasound applications. The fabrication techniques used are standard silicon micromachining procedures which lend themselves to batch fabrication and low cost manufacture.

For these electrostatic transducers to be useful, a number of issues must be addressed. One important concern is that the silicon nitride membrane will fatigue over time limiting the lifetime of the device. The peak displacement for the 100 μm period devices was approximately 3000 Å with 100 Volt bias and 16 V peak to peak signal. This corresponds to a strain of $2 \cdot 10^{-6}$. The fracture strain for silicon nitride[11] is $3.6 \cdot 10^{-2}$. Thus, we are operating well below the fracture limit and we would not expect fatigue to be a significant problem. The devices were ran for well over 300 hours with no measurable degradation in sensitivity or resonant frequency.

One problem with micromachined structures is their tendency to become contaminated when left open to the air. Water vapor, dust particles and other air-borne contamination get into the small spaces and prevent the devices from working. Because our devices have a very small (~ 3 μm) opening to the environment, we did not observe this problem. The transducers were left open in a dirty lab environment for weeks with no sign of contamination. This is an important feature of these transducers for enabling them to be usable in air-borne applications.

One advantage of electrostatic transducers over piezoelectric devices is there temperature sensitivity. PZT based transducers are very sensitive to temperature and can only by used near room temperature. Electrostatic devices are only limited by the melting point of the materials used and by the different thermal expansion of the materials used. For the devices described here, this upper temperature limit is approximately 400 °C. We tested the temperature behavior by placing a soldering iron tip on the sample during operation. There was no effect on the acoustic signal after 30 seconds of contact with the soldering iron tip. This is another large advantage of electrostatic transducers over conventional piezoelectric devices.

References:

1. J. Borwick, *Loudspeaker and Headphone Handbook*, Butterworth and Co., 1988

2. W.P. Mason, *Electromechanical Transducers and Wave Filters*, New York, D. Van Nostrand Company, 1942, pp. 163-165, 193-195

3. D.W. Schindel and D.A. Hutchins, "Capacitance Devices for the Controlled Generation of Ultrasonic Fields in Liquids," Proceedings of the IEEE Ultrasonics Symp., Ed: B.R. McAvoy (Institute of Electrical & Electronics Engineers, Inc., New York, 1991).

4. M. Rafiq and C. Wykes, "The performance of capacitive ultrasonic transducers using v-grooved backplates," Measurement Science Technology, 1991, Vol. 2, 168-174

5. H. Carr and C. Wykes, " Diagnostic measurements in capacitive transducers," Ultrasonics, 1993, Vol. 31, n. 1, pg. 13-20

6. Private Communications with S.P. Sandejas, Ginzton Laboratory, Stanford University, Stanford CA 94305

7. C-K Hsieh, Ph.D. Dissertation, Stanford Univeristy, 1993

8. D. Royer and E. Dieulesant, "Optical Probing of the Mechanical Impulse Response of a Transducer", Applied Physics Letters, Vol. 49 (17), October 27, 1986.

9. G.S. Kino, "Acoustic Waves," Prentice Hall, Inc., Englewood Cliffs, New Jersey, 1987

10. K. Peterson, "Silicon as a Mechanical Material," Proceedings of the IEEE-70 (5), 420 (1982)